ELSEVIER

International Journal of Mass Spectrometry 177 (1998) 83–89

International Journal of Mass Spectrometry

Mass spectra of $Fe(CO)_5$ using Fourier transform mass spectrometry (FTMS) and laser induced thermal desorption FTMS with electron ionization, charge exchange, and proton transfer

M. Noel Rocklein, Donald P. Land*

Department of Chemistry, University of California, Davis, CA 95616, USA

Received 1 March 1998; accepted 13 April 1998

Abstract

Fourier transform mass spectrometry is used with chemical ionization to observe iron pentacarbonyl molecules in an ultra-high vacuum system. Mass spectra are obtained from molecules desorbed from a cold Pd(111) surface using laser-induced thermal desorption (LITD) and directly from $Fe(CO)_5$ vapors. A variety of ions are formed when using 70 eV electrons, including some molecular ion. Charge exchange using Ar^+ and Xe^+ produces fewer fragment peaks but no molecular ion. Very little fragmentation occurs to the organometallic when using CH_5^+ for proton-transfer reactions. The proton transfer-LITD spectrum does, however, show an unexpected, nonprotonated iron tricarbonyl cation, presumably due to desorption of a surface-activated species. (Int J Mass Spectrom 177 (1998) 83–89) © 1998 Elsevier Science B.V.

Keywords: Laser-induced thermal desorption; Chemical ionization; Iron pentacarbonyl; Proton transfer; Charge exchange

1. Introduction

Iron pentacarbonyl has been the subject of a variety of mass spectrometric studies. Ionization and/or fragmentation has been achieved by collisions with electrons for cation [1–4] or anion [5–7] formation, with chemical reagents for protonation [8,9] or hydride formation [10], with low ionization energy species (such as potassium) for anion formation [5], and with thermally energized neutrals for unimolecular decomposition [11]. Nonfragmented cation species have been dissociated following collisions with neutrals [12,13] or after acceleration into instrument walls [14,15], as has the protonated product [8]. With the eventual goal of describing the thermal surface chemistry of iron pentacarbonyl, reported here are the first post-ionized laser-induced thermal desorption (LITD) mass spectra of a metal carbonyl. Soft-ionization techniques are explored in this work so future decomposition studies involving metal organics on a variety of surfaces may be made by using nonfragmented desorption products. Chemical ionization of laser-desorbed neutrals has been demonstrated by others in a Fourier transform mass spectrometer [16].

*Corresponding author.

Owing to late submission, this paper could not be included in the special issue in honour of Bob Taft, International Journal of Mass Spectrometry, Volume 175/1–2.

PII S1387-3806(98)14039-3

In this article, we present gas-phase and surface-desorbed spectra of $Fe(CO)_5$ obtained using Fourier transform mass spectrometry (FTMS) and LITD-FTMS. The basic principle of the LITD experiment is that a localized area of surface is heated so quickly that the predominant reaction of the adsorbed species is determined more by the entropy than by the enthalpy of activation; thus, at high temperatures, desorption often becomes favored over various thermal decomposition pathways. Ionization of gas-phase molecules and LITD neutrals is accomplished by electron ionization (EI) and by chemical ionization (CI) methods—charge exchange reactions occur following collisions of $Fe(CO)_5$ with argon or xenon ions and proton transfer reactions occur following collisions of $Fe(CO)_5$ with CH_5^+.

2. Experimental

Iron pentacarbonyl (Aldrich Chemical Co., Milwaukee, WI) was transferred under nitrogen to a foil-wrapped glass bulb and sealed from air by one viton O-ring (when closed) or two buna O-rings (when connected). This was attached to a stainless steel, diffusion-pumped foreline (base-pressure $< 5 \times 10^{-5}$ Torr) with a viton ultra-Torr fitting. Freeze–pump–thaw cycles were performed as needed using a dry-ice/acetone bath and the vapors sealed entirely in stainless steel showed no significant degradation when held overnight. After several foreline evacuations, the attached convectron gauges were rendered useless and were replaced with an ion gauge and an isolable convectron gauge.

The ultrahigh vacuum system (UHV, base-pressure $< 2 \times 10^{-10}$ Torr), the 1064 nanometer Nd:YAG laser, and the FTMS cubic ion analyzer cell have been described elsewhere [17]. A solenoid pulsed valve (General Valve Corp., Fairfield, NJ), located just outside the main field of the electromagnet used for FTMS, has been attached with a mini-conflat flange to a 1/4 in. stainless steel tube that was welded through a vacuum flange and bent directly towards the analyzer cell. In these experiments, the valve is typically backed by 1 Torr of reagent gas, and opening of the 0.8 mm orifice for 3.5 ms produces a large pressure surge ($\gg 10^{-6}$ Torr) in the cell that is then pumped to below 3×10^{-8} Torr within 2 s when using argon (sample and cooling arm at room temperature). Ions are formed near the start of this event by electron ionization and remain trapped within the analyzer cell by the magnetic field and by trapping plate voltages. Chemical ionization occurs as these ions are allowed to react with background gases or with laser-desorbed neutrals. Methane was purchased from Matheson Gas Products, Newark, CA at 99.99% purity and research grade argon was purchased from Spectra Gases, Inc., Vista, CA. Palladium single crystals were purchased from Princeton Scientific Corp., Princeton, NJ (Fig. 5–7) and from Aremco Products, Inc., Ossining, NY (Fig. 8). Both were polished with 0.05 μm alumina, were within 3 deg of the 111 face, and were freed of sulfur contamination by repeated sputter/anneal cycles. Temperature ramps to 850 K in ca. 10^{-6} Torr of oxygen were used to remove residual surface carbon. Surface exposures and LITD experiments were conducted at temperatures below 100 K. The reported exposures and backfill pressures are not corrected for ion gauge sensitivity or variable CO partial pressures. Unless otherwise noted, Fourier transform spectra were obtained using a 1/2 Hanning apodization function, 64 K data points, 2 MHz analog-to-digital converter (ADC) rate, with a magnetic field strength of 0.6 Tesla.

3. Results and discussion

The fragmentation pattern of $Fe(CO)_5$ following electron bombardment has been reported [1–4] and Fig. 1 shows a typical spectrum obtained with our FTMS at electron energies of 70 eV. Unfortunately, literature has been sparse in reporting CO concentrations, and a criterion for "clean" $Fe(CO)_5$ is difficult to establish. At 70 eV, Zaera [18] reported a $CO^+/Fe(CO)_5^+$ signal ratio of 280. Foster and Beauchamp [9] observed ion/molecule reactions in 2×10^{-6} Torr of $Fe(CO)_5$ by monitoring ion abundances versus time following a 6 ms, 70 eV electron beam pulse. Extrapolation to "0"ms reaction time shows a CO^+/Fe^+ ratio

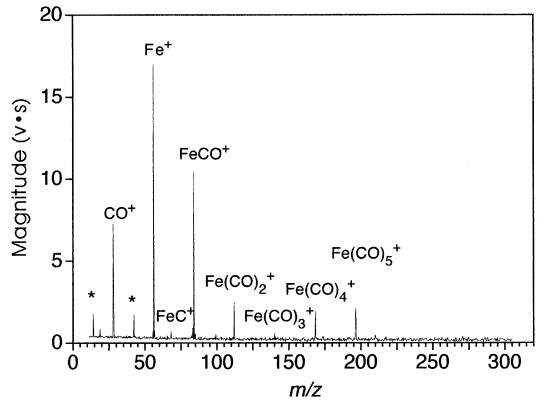

Fig. 1. Gas phase electron ionization Fourier transform mass spectrum of $Fe(CO)_5$ at 3.3×10^{-9} Torr by using 8 μA of 70 eV electrons for 30 ms. Peaks labeled with an asterisk are considered to be harmonic artifacts as determined by ion ejection experiments. When the spectrum is expanded, an harmonic of m/z 56 can be seen near m/z 28, appearing 0.05 u to the right of the larger CO^+ peak.

to be, approximately, 1.2. In an effort to make reproducible exposures, Henderson et al. [19] describe an oxygen pretreatment to the foreline and doser assembly to reduce decomposition reactions occurring on the doser walls and possibly on other UHV wall sites. They obtain a CO^+/Fe^+ ratio of about 1.5, at undisclosed electron energies (from Fig. 5 of [19], at middose). At 30 eV, Foffani et al.'s data [2] showed a CO^+/Fe^+ ratio of about 0.16 and attributed some of that CO intensity to the direct ionization of free CO since the appearance energy for CO^+ was the same as the CO ionization energy. Finally, at 21.2 eV (584 Å), Distefano reports a ratio of 0.047, attributing all intensity to free CO formed by decomposition in the inlet or from sample impurity [20]. Clearly, ionization energies play a significant role in CO^+ observation and production, especially considering the attenuated iron signal at low energies due to reduced fragmentation.

Significant, however, is the quantity and variance of CO seen under ultrahigh vacuum conditions. An oxygen pretreatment to the chamber of 5×10^{-8} Torr for 5 min is helpful in minimizing CO levels, although the CO^+ intensity still grows in with time, as might be expected if the deposited film or species allows for autocatalysis [19,21,22]. The relative CO concentration shown in Fig. 1 can further be reduced by increasing the pressure. This also suggests a limited number of UHV sites active in $Fe(CO)_5$ decomposition. These factors should be considered when conducting surface exposures or making conclusions about the origins of surface-adsorbed CO. Other spectral changes, distinct from above, are observed at higher pressures (approaching 2×10^{-7} Torr), including a significant decrease in the $Fe^+/Fe(CO)^+$ ratio and a continued decrease in the CO^+ concentration. This, however, is due to ion/molecule collisions that occur during the 50 ms reaction time after ionization and before detection, and not necessarily to changes in gas-phase composition; in the analyzer cell, CO^+ can undergo charge-exchange reactions with background $Fe(CO)_5$ to produce significant amounts of $Fe(CO)^+$ and $Fe(CO)_2{}^+$ [9].

Absolute signal intensities for gas phase EI spectra can be increased to a finite extent by (1) increasing the pressure, (2) increasing the temporal width of the ionizing pulse, and (3) increasing the electron current through the cell. At high ion densities, however, space-charge effects create signal instability. For LITD/EI experiments (at a given surface coverage and laser power density), only option 3 offers a potential to enhance signal intensities—until electron densities reduce trapping efficiencies and high filament currents warm cell plates, etc., causing an increase in background pressures. Although the absolute ion intensities are shown in all of the displayed spectra, a comparison between intensities is not relevant due to the experimental differences required to obtain them.

Because the ionization energies of $Fe(CO)_5$, CO, Ar, and Xe are 7.95, 14.01, 15.76, and 12.13 eV [23], respectively, a charge exchange between the ionized reagent gas and the metal carbonyl neutral may deposit approximately 7.8 eV using argon or 4.2 eV using xenon. Figure 2 shows iron pentacarbonyl's cracking pattern following charge exchange with Ar^+. All fragments are due to charge exchange and are not remnants of the ionization event, as proved by the following: the rf ejection voltages were increased until all ions except m/z 40 were successfully ejected, after which the remaining Ar^+ ions were allowed to react with the ambient background; subsequent ejec-

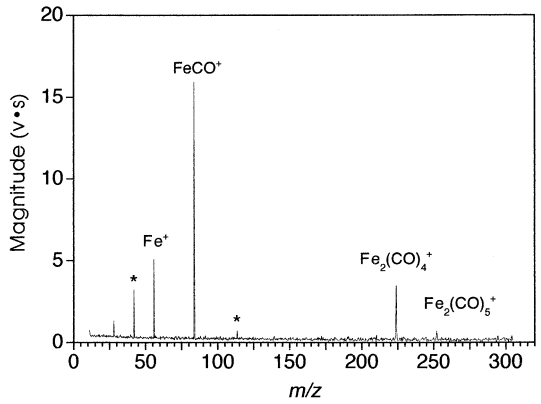

Fig. 2. Gas phase charge exchange Fourier transform mass spectrum of $Fe(CO)_5$ at 1.9×10^{-8} Torr by using Ar^+, 1600 ms reaction time.

tion of Ar^+ at progressively longer times showed all peaks to grow in with reaction time. By precedent, a whole series of clusters can be generated through ion–molecule collisions [9] and the observed $Fe_2(CO)_4^+$ and $Fe_2(CO)_5^+$ clusters at m/z 224 and 252 indicate the early stages of this process. When xenon ions are used for charge exchange, as shown in Fig. 3, the $Fe(CO)_2^+$ and $Fe(CO)_3^+$ ions initially formed react with background neutrals of produce primarily $Fe_2(CO)_6^+$ clusters through a single or double decarbonylation. Excess reagent ions (Xe^+) were not ejected. Peaks labeled with an asterisk are

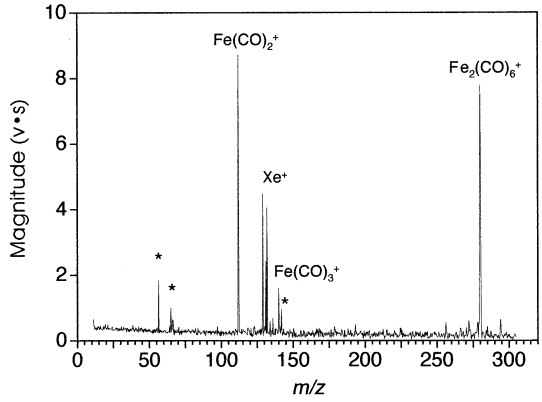

Fig. 3. Gas phase charge exchange Fourier transform mass spectrum of $Fe(CO)_5$ at 6.2×10^{-9} Torr by using Xe^+, 11 s reaction time.

not considered to be real mass-to-charge ratio signals; when a significant portion of the ion packet is formed off of the center axis of the analyzer cell, the Fourier transform may detect signals at integer harmonics of the cyclotron frequency [24]. This, of course, makes spectral analysis more difficult because multiply charged ions or singly charged ions of masses at fractional integers could be responsible for the observed peaks. For example, signals that might be misconstrued as "Xe^{4+}," "Xe^{3+}," and "Xe^{2+}" were observed at 1.5×10^{-8} Torr of xenon, which suggest the isotope peaks near m/z 65 in Fig. 3 to be harmonic artifacts rather than "Xe^{2+}" as Xe^{4+} cannot be created from 70 eV electrons under single interaction conditions. Further, these peaks were not ejected from Fig. 3 by the multiple ejection sweeps employed through this mass range. The peak at m/z 28 in Fig. 2 is probably a harmonic of m/z 56, although charge transfer to free CO is energetically feasible.

Ionizing methane during the pulsed-valve event quickly forms and traps a large concentration of CH_5^+ and $C_2H_5^+$ ions within the analyzer cell, both of which are capable of protonating $Fe(CO)_5$. The proton affinities of $Fe(CO)_5$, C_2H_4, CO, and CH_4 are 8.7, 7.0, 6.2, and 5.7 eV [25], respectively, and are used for heat of reaction calculations. By using only CH_5^+ reagent ions for organometallic protonation ($\Delta H_{rxn} = -3.0$ eV), a small degree of decarbonylation occurs to produce $Fe(CO)_4H^+$ at m/z 169, as seen in Fig. 4. Although $C_2H_5^+$ would certainly produce less fragmentation ($\Delta H_{rxn} = -1.7$ eV), it is not useful for CO protonation ($\Delta H_{rxn} = +0.8$ eV) whereas CH_5^+ is capable of protonating any of the decarbonylated neutrals, and CO as well ($\Delta H_{rxn} = -0.5$ eV). Currently, the absence of a COH^+ peak at m/z 29 is not a direct measure of sample purity as the cross section for CO protonation is probably less than that for iron pentacarbonyl. Excess CH_5^+ reagent ions were not ejected for this spectrum.

The LITD spectrum of $Fe(CO)_5$ on cold Pd(111) using electron ionization is shown in Fig. 5. The lower $Fe^+/Fe(CO)^+$ ratio observed might indicate that desorbing molecules remain internally cold, as compared to the room temperature spectrum in Fig. 1. However, the relative loss of the parent ion and

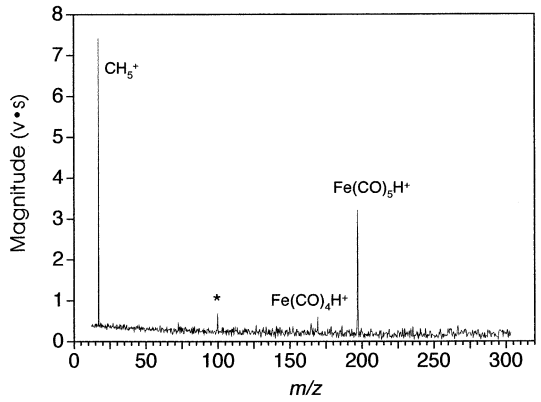

Fig. 4. Gas phase proton transfer Fourier transform mass spectrum of $Fe(CO)_5$ at 4.4×10^{-9} Torr by using CH_5^+, 1000 ms reaction time.

$Fe(CO)_4^+$ indicate otherwise, assuming $Fe(CO)_5$ to be the only iron-containing, laser-desorption product. Again, the need for a soft ionization technique arises. The loss of $Fe(CO)_4^+$ in the LITD spectrum might also be due to the lack of any gas-phase $Fe(CO)_5$ interactions with the hot rhenium EI filament to form $Fe(CO)_4$. Pignataro and Lossing [21] write that this moiety is even more susceptible to catalytic decomposition than is $Fe(CO)_5$, and that poisoning of any iron films (. . . or UHV wall sites) with O_2 or CS_2 increases $Fe(CO)_4$, $Fe(CO)_5$, and the $Fe(CO)_4^+/Fe(CO)_5^+$ ratio. The increased CO^+ signal is most probably due to background/surface accumulation accrued during the dose, but may also include catalytic activation from the Pd(111) surface at cold temperatures. Such a notion has been proposed for $Fe(CO)_5$ on the 111 [26] and polycrystalline [27] surfaces of platinum.

Using trapped Ar^+ for charge exchange, the LITD mass spectrum shown in Fig. 6 is practically identical to the gas-phase spectrum (Fig. 2), excluding the high mass, ion/molecule collision products discussed above. The actual strategy for obtaining a large signal intensity with about ±10% shot-to-shot stability is a compromise between maximizing the reagent ion density and reducing that density to discourage axial escape of the products and spurious space-charge effects. Admittedly, the chemical ionization experiments are more difficult than electron ionization experiments because successive scans are delayed by 2–5 s, making it difficult to relate tuning parameters with their effect.

A generous, multilayer exposure observed by LITD-FTMS using proton transfer from CH_5^+ is shown in Fig. 7, and is roughly estimated at 140 Langmuir. This includes an uncalibrated enhancement of about 30 (for this experiment only, the sample was placed directly in front of the doser tube) and division by 4.2 to correct for ion gauge sensitivities [28,29]. A protonated, singly decarbonylated product appears at m/z 169, and is suspected to arise from the protonated parent since it is also present in gas-phase

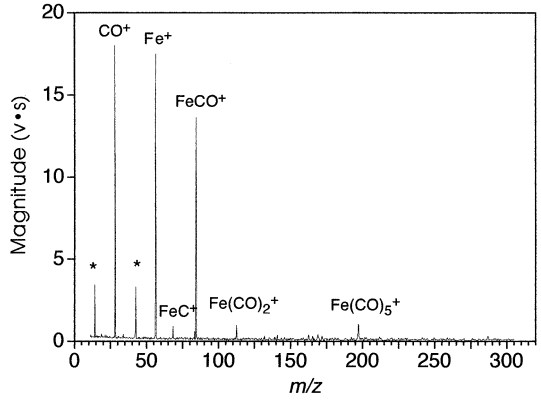

Fig. 5. LITD electron ionization Fourier transform mass spectrum (32 K data points) of $Fe(CO)_5$ using 20 μA of 70 eV electrons; 15 L (uncorrected) on palladium at <100 K.

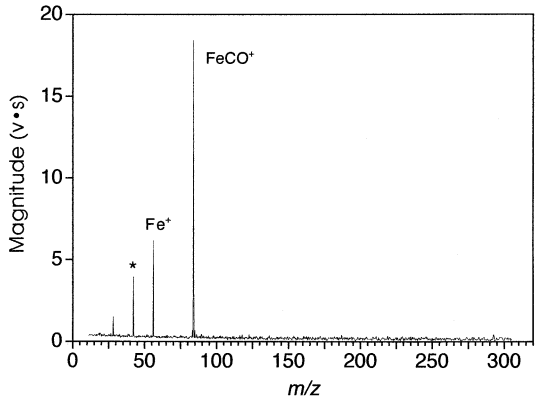

Fig. 6. LITD charge exchange Fourier transform mass spectrum of $Fe(CO)_5$ using Ar^+; 40 L (uncorrected) on palladium at <100 K.

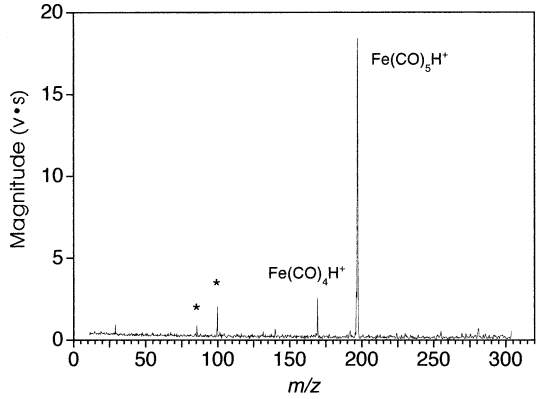

Fig. 7. LITD proton transfer Fourier transform mass spectrum of $Fe(CO)_5$ using CH_5^+; large exposure at <100 K.

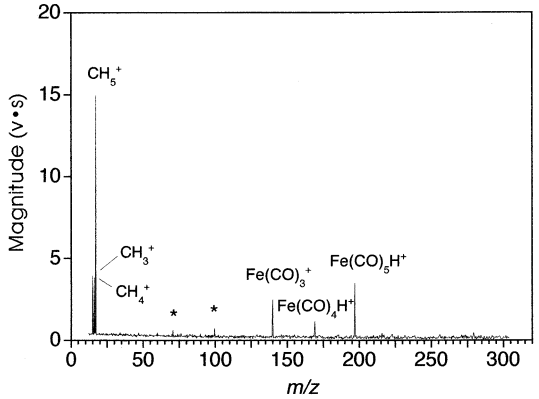

Fig. 8. LITD proton transfer Fourier transform mass spectrum of $Fe(CO)_5$ using CH_5^+; 40 L (uncorrected) exposure at <90 K.

fragmentation (Fig. 4) at longer delays. Reagent ions (CH_5^+) have been ejected prior to excitation and detection. The peaks near 86 and 100 are again considered harmonic artifacts of the heavier peaks and the peak at *m*/*z* 29 may be either COH^+ or residual $C_2H_5^+$ from incomplete ejection.

A significantly smaller exposure was made for comparison. Although visible in Fig. 8, the fragment at *m*/*z* 169 was not detectable at 5 ms or less, following the laser pulse. This suggests that $Fe(CO)_4H^+$ formation is not due to the direct protonation of $Fe(CO)_4$ desorbing from the surface or formed by laser induced fragmentation. Rather, this suggests that $Fe(CO)_4H^+$ formation is a rate-limited dissociation process following protonation of $Fe(CO)_5$.

Surprisingly, Fig. 8 shows a dramatic peak at *m*/*z* 140 which is barely discernible in Fig. 7 and is attributed to $Fe(CO)_3^+$. It is not due to direct ion desorption since no cations were detectable following a laser shot with the electron beam turned off in any of the EI or CI experiments. Low energy (12 eV) collision induced dissociation experiments with argon have shown that $Fe(CO)_5H^+$ will fragment to produce the whole range of protonated, decarbonylated products [8]. Therefore, a typical, thermally excited, CI fragmentation process is expected to produce only protonated products (i.e. at *m*/*z* 141), as would a proton transfer reaction to free $Fe(CO)_3$. It may be that the desorbing species ($Fe(CO)_5$, $Fe(CO)_4$, or $Fe(CO)_3$) were chemisorbed and leave the surface in some electronically activated state which allows for radical dissociation following CH_5^+ collision. Dissociation products might include neutral CO, H·, COH·, or even adduct species ($C_3O_2H_5$·?). Alternatively, a charge transfer from CH_5^+ might produce CH_3· and H_2. Due to the uniqueness of the $Fe(CO)_3^+$ fragment, a charge transfer from either CH_4^+ [$I(CH_4) = 12.6$ eV) or CH_3^+ ($I(CH_3$·$) = 9.83$ eV] [23] to ground-state $Fe(CO)_5$ is not suspected, depositing roughly 4.6 or 1.9 eV, respectively. This is because the loss of three carbonyls from $Fe(CO)_5^+$ requires less than 3 eV and the first decarbonylation requires less than 1.2 eV [12,20,30]. The *m*/*z* 140 peak was equally prominent from both solid samples at similar exposures.

Proton transfer coupled with LITD-FTMS may show an interesting surface phenomenon that electron ionization and charge exchange do not. If correct, this could be an exciting probe that immediately describes which molecules are resting in an activated precursor state. Factors that change this distribution would lend insight into the nature of surface activity. Two mechanisms involving an *activated* iron carbonyl moiety have been proposed to explain the $Fe(CO)_3^+$ signal observed during the LITD proton transfer experiments: the CH_5^+ reagent ion (1) accepts an electron instead of acting as a protonating agent, or (2) donates a proton or forms an adduct, after which the product

dissociates a lone hydrogen or hydrogen-containing radical. Further, because only a small amount of $Fe(CO)_3^+$ was generated from the condensed phase spectrum (Fig. 7), the activation is suspected to be a surface phenomena and not a thermal- or photon-induced electronic excitation.

4. Conclusion

Several techniques for ionizing iron pentacarbonyl have been explored in a Fourier transform mass spectrometer. Unlike EI, charge exchange produced no parent ion; Ar^+ produces mostly Fe^+ and $Fe(CO)^+$, while Xe^+ generates $Fe(CO)_2^+$ and $Fe(CO)_3^+$. Proton transfer using CH_5^+ produces primarily $Fe(CO)_5H^+$ with some $Fe(CO)_4H^+$. Background carbon monoxide levels can be reduced by an oxygen pretreatment to the chamber and by increasing the pressure relative to the pumping speed. Ion/molecule reactions were found to occur in the 10^{-8} Torr regime under conditions of high ion densities and moderate reaction times ($\geq$50 ms) and in the 10^{-9} Torr regime at longer reaction times ($\geq$1000 ms). Chemical ionization methods were also incorporated into the LITD experiment. It does appear that EI is better suited to detect low (submonolayer) coverages, although efforts to improve CI detection limits (such as increasing reagent ion densities or increasing laser spot-size) may prove successful. Proton transfer, however, does produce significantly less fragmentation, even in LITD, and could therefore be useful in identifying the nascent laser-desorbed species for compounds, such as organometallics, which typically give very weak molecular ion signals under EI.

Acknowledgement

The authors are thankful for funding from the National Scholarship Foundation for support of this work, under Grant No. CHE-9612732.

References

[1] R.E. Winters, R.W. Kiser, Inorg. Chem. 3 (1964) 699.
[2] A. Foffani, S. Pignataro, B. Cantone, F. Grasso, Z. Phys. Chem. Frankfurt 45 (1965) 79.
[3] D.R. Bidinosti, N.S. McIntyre, Can. J. Chem. 45 (1967) 641.
[4] G.A. Junk, H.J. Svec, Z. Naturforsch. B 23 (1968) 1.
[5] R.N. Compton, J.A.D. Stockdale, Int. J. Mass Spectrom. Ion Phys. 22 (1976) 47.
[6] P.C. Engelking, W.C. Lineberger, J. Am. Chem. Soc. 101 (1979) 5569.
[7] R.N. McDonald, A.K. Chowdhury, M.T. Jones, J. Am. Chem. Soc. 108 (1986) 3105.
[8] C.E. Allison, J.A. Cramer, C.E.C.A. Hop, J.E. Szulejko, T.B. McMahon, J. Am. Chem. Soc. 113 (1991) 4469.
[9] M.S. Foster, J.L. Beauchamp, J. Am. Chem. Soc. 97 (1975) 4808.
[10] K.R. Lane, R.R. Squires, Polyhedron 7 (1988) 1609.
[11] K.E. Lewis, D.M. Golden, G.P. Smith, J. Am. Chem. Soc. 106 (1984) 3905.
[12] R.H. Schultz, K.C. Crellin, P.B. Armentrout, J. Am. Chem. Soc. 113 (1991) 8590.
[13] R.B. Cody, D.A. Weil, Abstracts of the 36th ASMS Conference on Mass Spectrometry and Allied Topics, San Francisco, 5–10 June 1988, ASMS, Santa Fe, NM, pp. 1332–1333.
[14] J.A. Castoro, P.V. Rucker, C.L. Wilkings, J. Am. Soc. Mass Spectrom. 3 (1992) 445.
[15] M.J. DeKrey, H.I. Kenttamaa, V.H. Wysocki, R.G. Cooks, Org. Mass Spectrom. 21 (1986) 193.
[16] J.P. Speir, G.S. Gorman, I.J. Amster, J. Am. Soc. Mass Spectrom. 4 (1993) 106, and references cited therein.
[17] D.P. Land, I.M. Abdelrehim, N.A. Thornburg, J.T. Sloan, Anal. Chim. Acta 307 (1995) 321.
[18] F. Zaera, J. Vac. Sci. Technol. A 7 (1989) 640.
[19] M.A. Henderson, R.D. Ramsier, J.T. Yates Jr., J. Vac. Sci. Technol. A 9 (1991) 2785.
[20] G. Distefano, J. Res. Natl. Bur. Stand., Sec. A 74A (1970) 233.
[21] S. Pignataro, F.P. Lossing, J. Organometal. Chem. 11 (1968) 571.
[22] F. Zaera, Langmuir 7 (1991) 1188.
[23] D.R. Lide (Ed.), CRC Handbook of Chemistry and Physics, CRC, Boston, 1991–1992.
[24] A.G. Marshall, P.B. Grosshans, Anal. Chem. 63 (1991) 215A.
[25] F.W. McLafferty, F. Turecek, Interpretation of Mass Spectra, Fourth, University Science Books, Mill Valley, 1993, pp. 343–345; for a more extended table of proton affinities see S.G. Lias, J.F. Liebman, R.D. Levin, J. Phys. Chem. Ref. Data 13 (1984), 695.
[26] F. Zaera, Surf. Sci. 255 (1991) 280.
[27] S. Sato, Y. Ukisu, Surf. Sci. 283 (1993) 137.
[28] J.E. Bartmess, R.M. Georgiadis, Vacuum 33 (1983) 149.
[29] J.W. Otvos, D.P. Stevenson, J. Am. Chem. Soc. 78 (1956) 546.
[30] K. Norwood, A. Ali, G.D. Flesch, C.Y. Ng, J. Am. Chem. Soc. 112 (1990) 7502.